Proceedings of the 10th International Conference on Biomedical Engineering and Systems (ICBES 23)
Brunel University, London, United Kingdom – August 03-05, 2023
Paper No. ICBES 161
DOI: 10.11159/icbes23.161

Classification of Auditory Oddball Evoked Potentials using Group Task Related Component Analysis

Bruno A. N. Couto[1], Adenauer G. Casali[1]
[1] Institute of Science and Technology, Federal University of São Paulo
R. Talim 330, São José dos Campos, Brazil
bruno.couto@unifesp.br; casali@unifesp.br

Abstract **-** Electroencephalographic (EEG) Evoked Potentials (EPs) have gained significant attention as promising tools for non-invasive investigation of a wide array of neurological and neuropsychiatric conditions. Progress in this area relies on the capacity to identify and automatically extract patterns of EPs that are reproducible at the group level. The present study explores the application of Group Task-Related Component Analysis (gTRCA), an innovative multivariate signal decomposition technique, to the characterization and classification of auditory evoked potentials. Using a publicly available dataset of auditory oddball EPs, we employed gTRCA to extract reproducible components of EEG recordings from 40 healthy subjects exposed to standard and deviant auditory stimuli in a mismatch negativity protocol. The extracted temporal patterns were then utilized as templates for classifying auditory oddball EPs in the standard or deviant classes based on their optimal alignment with the primary gTRCA components triggered by the respective type of stimulation. Our results confirmed that gTRCA was able to reliably extract significantly reproducible components ($p<0.001$) of auditory EPs with spatiotemporal attributes that were coherent with the type of stimulation. Furthermore, the extracted temporal patterns were shown to be robust and sufficiently distinct to be used in the classification of auditory EPs, achieving median accuracy of 90%. Our findings posit gTRCA as a powerful tool for optimizing scientific and clinical studies exploring novel markers for various clinical conditions associated with alterations in EEG evoked potentials.

Keywords**:** EEG, Auditory Oddball Evoked Potentials, Mismatch Negativity, gTRCA, Dimensionality Reduction, Pattern Recognition

1 1. INTRODUCTION

Electroencephalographic (EEG) evoked potentials (EPs) are among the most widely used tools in the field of neuroscience and have been applied in the non-invasive investigation of various clinical conditions [1]. Abnormalities in the characteristics of evoked components elicited by different types of stimuli appear as potential candidates for supporting the identification of several diagnostically challenging pathologies such as dementia and neurodegenerative diseases [2, 3], depression [4], schizophrenia [5], and autism spectrum disorder [6]. However, the development of such diagnostic tools hinges on the ability to extract patterns from evoked signals that are reproducible across stimuli and individuals and that can be employed in the automatic classification of EPs in different conditions of interest.

Recent advances have been made in multivariate analysis methodologies with the intention of optimizing the detection of reproducible EEG components at the group level [7] - [9]. Among these techniques, the Group Task-Related Component Analysis (gTRCA) stands out for having two characteristics that make it particularly interesting for applications in EPs: gTRCA identifies components that are simultaneously reproducible across both dimensions of interest (stimuli and subjects) and is flexible enough to accommodate spatial variations between subjects, making it ideal for group-level analyses of EEG recordings. Despite its potential, gTRCA has been tested only on steady-state EPs [10], leaving its application to other types of EPs still unexplored.

Among the various types of evoked potentials, auditory oddball EPs recorded in mismatch negativity (MMN) protocols have recently attracted significant interest, shedding light on numerous neural mechanisms underpinning auditory processing, plasticity, and pre-attentional processes [11, 12]. MMN protocols entail the presentation of a deviant auditory stimulus, distinct from other more frequent or standard stimuli, and elicit a characteristic response that can be captured in EEG recordings. This stimulus-induced response manifests as a depolarization in the fronto-central and central EEG electrodes, with peak activity typically observed within a time frame of 150 to 250 ms after the stimuli [11]. A notable advantage of these protocols is their broad applicability in examining diverse neuropathologies and clinical conditions where alterations in auditory processing are significant [13, 14], such as early stage psychosis [15], bipolar disorder [16], ageing [17],

functional outcomes in patients with traumatic brain injury [18], autism [19], and even as a prospective predictor of mental health issues in children [20].

In the present study we explore the hypothesis that gTRCA can be applied to auditory oddball EPs in healthy subjects to effectively extract temporal and spatial patterns that are reproducible at the group level and that can be used to automatically discriminate between the two types of stimuli presented in the MMN protocol.

2 2. MATERIAL AND METHODS

2.1 2.1 Data and Preprocessing

The current investigation employed a publicly available database furnished by Kappenman and collaborators [21], which includes pre-processed and segmented EEG recordings from 40 neurotypical, healthy subjects (25 females; 15 males; ages spanning from 18 to 30) subjected to a passive auditory oddball paradigm as a way to assess mismatch negativity. Within this paradigm, standard (80 dB, p=0.8) and deviant (70 dB, p=0.2) auditory stimuli were presented via speakers while participants watched a silent video [21]. Each participant received 800 stimuli in the standard condition and 200 stimuli in the deviant condition.

For the analysis performed in this study, we extracted the pre-processed EEG signals of all 40 subjects. As described in the ERP Core dataset, EEG data were acquired at a sampling rate of 1024Hz using a Biosemi ActiveTwo system with 30 channels (28 EEG + 2 EOG) positioned in compliance with the International 10/20 System. The pre-processed signals used in this study had previously undergone the following pre-processing steps [21]: anti-aliasing filter and downsampling to 256 Hz, re-referencing to the average of P9 and P10, DC offset removal, artifact removal via Independent Component Analysis and visual inspection, segmentation in epochs (trials) from -200ms to 800ms relative to the stimulus onset, and baseline correction. Finally signals were low-pass filtered with a 20 Hz cut-off. As result of the preprocessing, evoked potentials were constructed with an average number of 534.95 ± 59.39 trials in response to the standard stimuli and 183.18 ± 21.14 trials in response to the deviant stimulus. Figure 1 provides a visual representation of the dataset, showing the grand average potentials (across all subjects) under each condition (standard and deviant).

3 2.2 METHODS

In this section, we describe the gTRCA approach used to extract reproducible components from evoked potentials [10], as well as the procedure employed to classify EPs by projecting them on the first gTRCA component of each group. All analyses delineated herein were conducted utilizing Python, in conjunction with the MNE library [22, 23]. The code used in this study is publicly available at GitHub [24].

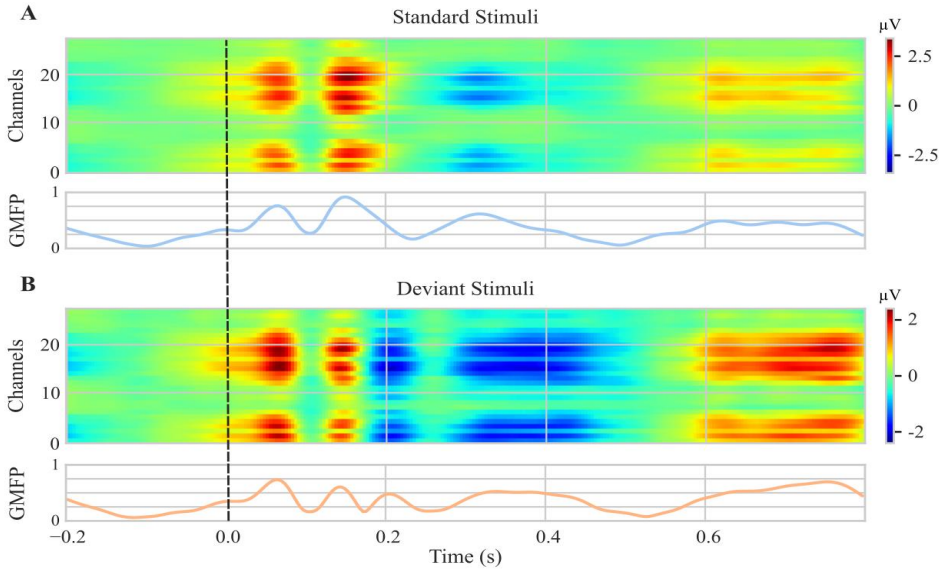

Figure 1: Grand average of EEG evoked responses for (A) standard auditory stimuli and (B) deviant stimuli across all 40 participants. The heatmaps display the average time-series across all trials and subjects for each EEG channel. The

curves beneath each image display the associated global mean field power (GMFP), calculated as the voltage root mean square across all channels.

3.1.1 2.2.1 Group Task-Related Component Analysis

Let an EEG epoch recorded in individual α (α = 1...A) be represented by the matrix $X_\alpha^k \in R^{n \times \tau}$, where k denotes the epoch or trial (k = 1...K), n the total number of EEG channels, and τ the epoch length (number of samples). Following Tanaka, in this section we operate under the assumption that n, τ, and K are consistent across subjects, but this restriction is assumed only for the sake of notational simplicity and can be disregarded in real applications [10].

The method developed by Tanaka for steady-state potentials starts from continuous EEG recordings that are used to calculate the global EEG covariance matrix, Q [10]. However, artifact-free continuous recordings are typically not available in EP protocols, as various artifact removal strategies are usually applied to the already segmented epochs. For this reason, we estimated the global EEG covariance from matrices $X_\alpha \in R^{n \times k\tau}$ with preprocessed trials of individual α concatenated along the temporal dimension. In these matrices, EEG channels were normalized to have zero mean and unit standard deviation. For each individual, a covariance matrix Q_α was then calculated as

$$Q_\alpha = \frac{1}{T} X_\alpha X_\alpha^\top \in R^{n \times n}. \quad (1)$$

The total covariance of the group $Q \in R^{nA \times nA}$ was then constructed as the block-diagonal matrix having Q_α (α = 1... A) as its submatrices.

The methodology of the gTRCA is grounded on the covariance matrix Q and in a matrix $S \in R^{nA \times nA}$ constructed as follows:

$$S_{\alpha,\alpha} = \frac{1}{(K-1)K\tau} \sum_{k,l=1;\, k \neq l}^{K} X_\alpha^{(k)} X_\alpha^{(l)\top} \in R^{n \times n} \quad (2)$$

$$S_{\alpha,\beta\ (\alpha \neq \beta)} = \frac{1}{K^2\tau} \sum_{k,l=1}^{K} X_\alpha^{(k)} X_\beta^{(l)\top} \in R^{n \times n} \quad (3)$$

The main diagonal of S (Eq. 2) quantifies the intrasubject reproducibility (average correlation across trials within each subject) and the off-diagonal elements (Eq. 3) measures the intersubject reproducibility (correlation across trials of different subjects). The main goal of gTRCA is to find spatial filters w_α that maximize S under the constraint of fixed EEG covariance, which result in components maximally reproducible both across trials and subjects. This problem can be formulated as a Rayleigh-Ritz eigenvalue problem, with solution $w \in R^{nA \times 1}$ given by

$$w = argmax\left(\frac{w^\top S w}{w^\top Q w}\right), \quad (4)$$

where w is formed by the column-wise concatenation of the individual spatial filters w_α.

The resulting eigenvectors w are subsequently sorted by their associated eigenvalues (λ), which measures the total strength of the component's reproducibility across trials and subjects. The correspondent gTRCA components $y_\alpha^{(k)} \in R^{1 \times \tau}$ are obtained by filtering the EEG with w_α, i.e., $y_\alpha^{(k)} = w_\alpha^\top X_\alpha^{(k)}$. Finally, the spatial maps $m_\alpha \in R^{n \times 1}$ associated with each component are calculated as $m_\alpha = Q_\alpha w_\alpha$ [10]. gTRCA components were normalized with zero mean and unit variance.

We tested the reproducibility of gTRCA components by comparing their eigenvalues to a distribution derived from surrogate data. This data was generated by randomly shifting trials along the temporal dimension across all channels and individuals [25, 26]. We created 1000 surrogates and components were considered significantly reproducible if they achieved a statistical level of $p<0.01$.

3.1.2

3.1.3 2.2.2 Classification of Evoked Potentials with gTRCA

To assess the capacity of gTRCA in classifying auditory evoked potentials, we extracted the first component of each stimulus type from a subset of individuals, which served as the training data for the classifier. The evoked potentials of the excluded individuals, designated as the test data, were then projected onto the gTRCA components using a spatial filter w_{A+1}. This filter was derived from the weighted sum of the filters $\{w_\alpha\}$ originating from the individuals in the training group ($\alpha = 1, \ldots, A$) as follows:

$$w_{A+1} = \frac{1}{2A\zeta} Q_{A+1}^{-1} U_{A+1} \sum_{\alpha=1}^{A} U_\alpha^\top w_\alpha, \quad (5)$$

where ζ corresponds to the Lagrange multiplier, $A+1$ corresponds to an individual in the test group with covariance matrix Q_{A+1} and $U \in R^{n \times \tau}$ corresponds to the EPs of the individuals of the training (U_α) and test (U_{A+1}) datasets. The parameter ζ was fixed by normalizing the projected evoked potential y_{A+1} of the test subjects to unit variance, where $y_{A+1} = w_{A+1}^\top U_{A+1}$.

The projected evoked potentials were compared with the corresponding mean gTRCA components derived from the training dataset for each condition. EPs from the test data were subsequently classified as either resulting from standard or deviant stimuli, depending on which corresponding component best fitted the projected EP. This fit was estimated by calculating the root mean square error (RMSE) between the two time series within the window of interest (150-250ms). The procedure was repeated 500 times, with individuals being randomly assigned to the training and test groups each time. The median rates of true positives for detecting the deviant condition, true negatives (for detecting the standard condition) and overall classifier accuracy were calculated across all repetitions.

4 3. RESULTS AND DISCUSSION

The application of Group Task Related Component Analysis to auditory oddball evoked potentials yielded two significant components for both experimental conditions ($p < 0.001$). In this study we concentrated our analysis on the first gTRCA component of each group, which are displayed in Figure 2.

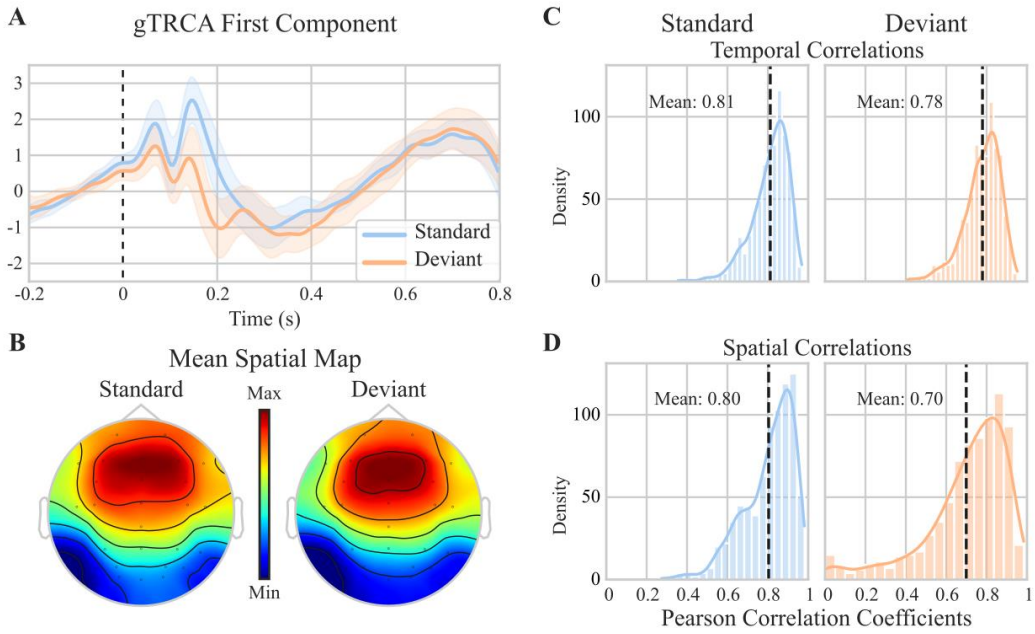

Fig. 2: Spatiotemporal characteristics of the first gTRCA component in a passive auditory oddball protocol. Panel (A) presents the temporal series of the first gTRCA component in response to standard (blue) and deviant (orange) auditory stimuli. The solid lines depict averages across subjects, with the shaded regions representing 1.5 standard deviations above and below the respective means. Panel (B) exhibits the average topographic distributions of the gTRCA scalp maps for each condition (standard on the left and deviant on the right). Panels (C) and (D) display the distributions of correlations across individuals' first components using the temporal series (temporal correlations, panel C) and spatial maps (spatial correlations, panel D). Temporal and spatial correlations were computed pairwise along individuals within the same condition. The black dashed line indicates the position of the mean correlation values for each condition (standard in blue, deviant in orange).

Consistent with the vast corpus of literature on passive auditory oddball evoked potentials [11, 14], we noted a clear divergence between the groups in the 150-250 ms span of the component time series. Specifically, a negative peak manifested around the 200 ms mark in the deviant condition, while an enhanced amplitude peak was apparent between 150 and 200 ms in response to standard stimuli (Figure 2A). The topographies of each component also exhibited the anticipated spatial patterns for MMN protocols, with activity predominantly concentrated in the fronto-central and central EEG electrodes (Figure 2.B). To evaluate the inter-subject reproducibility of the first component, we computed pairwise Pearson's correlation coefficient across subjects within groups, both for the components' time-series (temporal correlation, Figure 2C) and spatial maps (spatial correlation, Figure 2D). The first gTRCA component exhibited a high degree of temporal correlation across subjects (mean ± standard deviation of 0.81 ± 0.09 and 0.78 ± 0.09, for the standard and deviant conditions, respectively). Importantly, a similarly high level of correlation was also observed across the spatial maps (0.80 ± 0.12 and 0.70 ± 0.21), despite the fact that the gTRCA approach relies solely on temporal correlations and imposes no constraints on the spatial distribution of components, which can emerge from different spatial filters for different subjects.

The high spatial correlation observed across subjects in Figure 2D suggests that the group-level reproducibility of the first gTRCA component is not the result of overfitting. To further investigate this hypothesis, we analyzed the temporal stability of the first component under reduction of the number of individuals (Figure 3A).

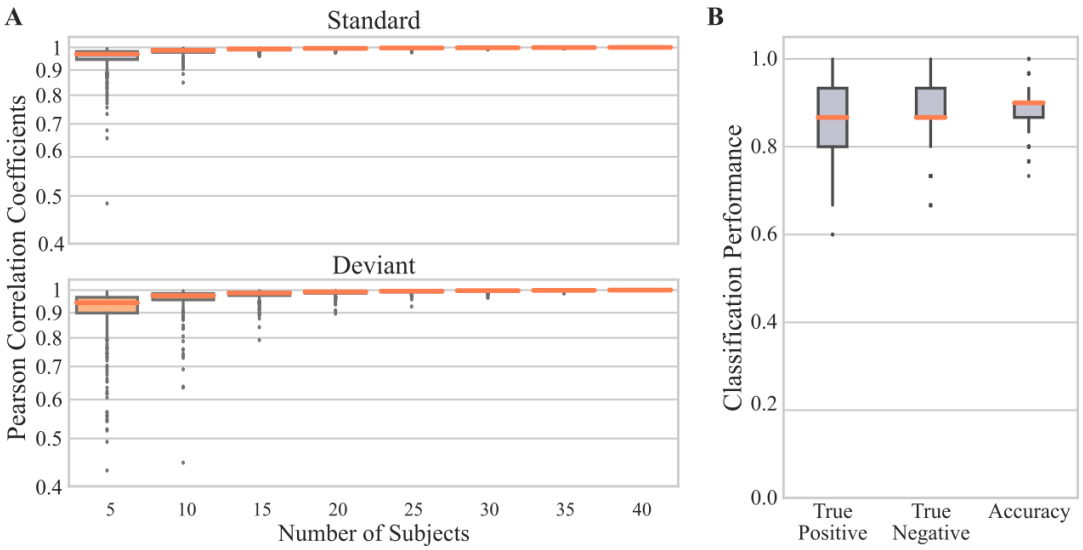

Fig. 3: Robustness and generality of the first gTRCA component in characterizing and classifying auditory oddball evoked potentials. Panel (A) presents the distribution of correlation values between the first gTRCA component obtained with the complete dataset and the same component extracted from subsets with a reduced number of individuals for both conditions (standard stimuli above, deviant below). The medians of the distributions for both conditions (standard and deviant) surpassed 0.95 with as few as 10 subjects and were above 0.995 with 25 subjects. Panel (B) displays the results of utilizing the components extracted with 25 subjects to classify the auditory EPs of the remaining 15 individuals. Classification power was measured in terms of true positive rates (deviant), true negative rates (standard) and overall accuracy. In this figure, box plots display medians, interquartile ranges and outliers for the distributions resulting from 500 repetitions.

For this analysis, Pearson's correlation coefficient was calculated between the components obtained with the complete dataset (40 individuals) and those derived from subsets formed by randomly removing 5 subjects at a time and repeated 500 times. The first gTRCA component displayed high levels of stability, with median correlations for both conditions reaching 0.995 for the removal of up to 15 subjects (medians and minimums values of correlations for the subset using 25 subjects were 0.997 and 0.977 for the standard condition and 0.995 and 0.926 for the deviant condition, respectively). This analysis attested that gTRCA can be used to optimize evoked potential protocols by identifying the minimum number of subjects needed to extract reproducible patterns at the group level.

As a final test of the generality of the method, we employed the first gTRCA component obtained from the subsets with 25 subjects (training data) to classify the auditory evoked potentials of the remaining 15 subjects (test data) as described in section 2.2.2. The temporal patterns extracted with gTRCA from the training dataset achieved a high level of accuracy (median value of 90%) in the test datasets despite the use of a simple best fit classifier (Figure 3B). This result suggests that the method can be useful to detect alterations in MMN components in conditions of clinical interest [13] - [20]. Future studies should investigate this hypothesis by combining gTRCA to other classification strategies.

5 4. CONCLUSION

In this study, we examined the use of gTRCA, an innovative multivariate signal decomposition technique, in characterizing auditory oddball evoked potentials derived from healthy individuals undergoing a mismatch negativity protocol. Our findings affirm the hypothesis that this method can extract components that are reproducible at the group level and exhibit the same spatiotemporal patterns as the EEG potentials evoked by

corresponding types of auditory stimuli. Moreover, we demonstrated here that the temporal patterns of gTRCA are robust enough to be extracted with a reduced number of subjects and are sufficiently specific to be used as templates in the classification of evoked potentials. These results carry potential applications not only in optimizing scientific and clinical studies, but also in developing diagnostic support tools for conditions associated with alterations in EEG evoked potentials.

6 ACKNOWLEDGMENTS

This study was financed in part by the Coordenação de Aperfeiçoamento de Pessoal de Nível Superior – Brasil (CAPES) – Finance Code 001.

7 REFERENCES

[1] R. F. Helfrich and R. T. Knight, "Cognitive neurophysiology: Event-related potentials," in *Handbook of Clinical Neurology*, Elsevier, 2019, pp. 543–558. doi: 10.1016/B978-0-444-64032-1.00036-9.

[2] N. Armanfard, M. Komeili, J. P. Reilly, R. Mah, and J. F. Connolly, "Automatic and continuous assessment of ERPs for mismatch negativity detection," in *2016 38th Annual International Conference of the IEEE Engineering in Medicine and Biology Society (EMBC)*, Orlando, FL, USA: IEEE, Aug. 2016, pp. 969–972. doi: 10.1109/EMBC.2016.7590863.

[3] O. J. H. Fustes, C. S. K. Kay, P. J. Lorenzoni, R. D.-P. Ducci, L. C. Werneck, and R. H. Scola, "Somatosensory evoked potentials in clinical practice: a review," *Arq. Neuropsiquiatr.*, vol. 79, no. 9, pp. 824–831, Sep. 2021, doi: 10.1590/0004-282x-anp-2020-0427.

[4] Y.-J. Tseng, R. Nouchi, and C.-H. Cheng, "Mismatch negativity in patients with major depressive disorder: A meta-analysis," *Clin. Neurophysiol.*, vol. 132, no. 10, pp. 2654–2665, Oct. 2021, doi: 10.1016/j.clinph.2021.06.019.

[5] J. M. Ford, V. A. Palzes, B. J. Roach, and D. H. Mathalon, "Did I Do That? Abnormal Predictive Processes in Schizophrenia When Button Pressing to Deliver a Tone," *Schizophr. Bull.*, vol. 40, no. 4, pp. 804–812, Jul. 2014, doi: 10.1093/schbul/sbt072.

[6] M. D. Bomba and E. W. Pang, "Cortical auditory evoked potentials in autism: a review," *Int. J. Psychophysiol.*, vol. 53, no. 3, pp. 161–169, Aug. 2004, doi: 10.1016/j.ijpsycho.2004.04.001.

[7] Hasenstab, K., Scheffler, A., Telesca, D., Sugar, C. A., Jeste, S., DiStefano, C., & Şentürk, D. (2017). "A multi-dimensional functional principal components analysis of EEG data". *Biometrics*, 73(3), 999–1009. doi: https://doi.org/10.1111/biom.12635.

[8] L. C. Parra, S. Haufe, and J. P. Dmochowski, "Correlated Components Analysis - Extracting Reliable Dimensions in Multivariate Data," *ArXiv180108881 Cs Stat*, Jan. 2019, Accessed: Jan. 24, 2022. [Online]. Available: http://arxiv.org/abs/1801.08881

[9] X. Zhuang, Z. Yang, and D. Cordes, "A technical review of canonical correlation analysis for neuroscience applications," *Hum. Brain Mapp.*, vol. 41, no. 13, pp. 3807–3833, Sep. 2020, doi: 10.1002/hbm.25090.

[10] H. Tanaka, "Group task-related component analysis (gTRCA): a multivariate method for inter-trial reproducibility and inter-subject similarity maximization for EEG data analysis," *Sci. Rep.*, vol. 10, no. 1, p. 84, Dec. 2020, doi: 10.1038/s41598-019-56962-2.

[11] R. Näätänen, P. Paavilainen, T. Rinne, and K. Alho, "The mismatch negativity (MMN) in basic research of central auditory processing: A review," *Clin. Neurophysiol.*, vol. 118, no. 12, pp. 2544–2590, Dec. 2007, doi: 10.1016/j.clinph.2007.04.026.

[12] R. Näätänen, "Mismatch negativity (MMN) as an index of central auditory system plasticity," *Int. J. Audiol.*, vol. 47, no. sup2, pp. S16–S20, Jan. 2008, doi: 10.1080/14992020802340116.

[13] Näätänen, R., Kujala, T., Escera, C., Baldeweg, T., Kreegipuu, K., Carlson, S., & Ponton, C. (2012). "The mismatch negativity (MMN) – A unique window to disturbed central auditory processing in ageing and

different clinical conditions," *Clin. Neurophysiol.*, 123(3), 424–458. doi: https://doi.org/10.1016/j.clinph.2011.09.020.
[14] M. I. Garrido, J. M. Kilner, K. E. Stephan, and K. J. Friston, "The mismatch negativity: A review of underlying mechanisms," *Clin. Neurophysiol.*, vol. 120, no. 3, pp. 453–463, Mar. 2009, doi: 10.1016/j.clinph.2008.11.029.
[15] Tada, M., Kirihara, K., Mizutani, S., Uka, T., Kunii, N., Koshiyama, D., Fujioka, M., Usui, K., Nagai, T., Araki, T., & Kasai, K. (2019). "Mismatch negativity (MMN) as a tool for translational investigations into early psychosis: A review," *Int. J. Psychophysiol.*, 145, 5–14. doi: https://doi.org/10.1016/j.ijpsycho.2019.02.009
[16] D. F. Hermens, K. M. Chitty, and M. Kaur, "Mismatch negativity in bipolar disorder: A neurophysiological biomarker of intermediate effect?," *Schizophr. Res.*, vol. 191, pp. 132–139, Jan. 2018, doi: 10.1016/j.schres.2017.04.026.
[17] C.-H. Cheng, W.-Y. Hsu, and Y.-Y. Lin, "Effects of physiological aging on mismatch negativity: A meta-analysis," *Int. J. Psychophysiol.*, vol. 90, no. 2, pp. 165–171, Nov. 2013, doi: 10.1016/j.ijpsycho.2013.06.026.
[18] H. Sun, Q. Li, X. Chen, and L. Tao, "Mismatch negativity, social cognition, and functional outcomes in patients after traumatic brain injury," *Neural Regen. Res.*, vol. 10, no. 4, p. 618, 2015, doi: 10.4103/1673-5374.155437.
[19] G. Di Lorenzo, A. Riccioni, M. Ribolsi, M. Siracusano, P. Curatolo, and L. Mazzone, "Auditory Mismatch Negativity in Youth Affected by Autism Spectrum Disorder With and Without Attenuated Psychosis Syndrome," *Front. Psychiatry*, vol. 11, p. 555340, Nov. 2020, doi: 10.3389/fpsyt.2020.555340.
[20] T. Aoi, T. X. Fujisawa, S. Nishitani, and A. Tomoda, "Mismatch negativity of preschool children at risk of developing mental health problems," *Neuropsychopharmacol. Rep.*, vol. 41, no. 2, pp. 185–191, Jun. 2021, doi: 10.1002/npr2.12168.
[21] E. S. Kappenman, J. L. Farrens, W. Zhang, A. X. Stewart, and S. J. Luck, "ERP CORE: An open resource for human event-related potential research," *NeuroImage*, vol. 225, p. 117465, Jan. 2021, doi: 10.1016/j.neuroimage.2020.117465.
[22] A. Gramfort, "MEG and EEG data analysis with MNE-Python," *Front. Neurosci.*, vol. 7, 2013, doi: 10.3389/fnins.2013.00267.
[23] Larson, Eric, Gramfort, Alexandre, Engemann, Denis A, Leppakangas, Jaakko, Brodbeck, Christian, Jas, Mainak, Brooks, Teon, Sassenhagen, Jona, Luessi, Martin, McCloy, Daniel, King, Jean-Remi, Goj, Roman, Favelier, Guillaume, Höchenberger, Richard, Brunner, Clemens, van Vliet, Marijn, Wronkiewicz, Mark, Holdgraf, Chris, Massich, Joan, … Luzpaz. (2023). "MNE-Python.". Zenodo, Feb. 23, 2023. doi: https://doi.org/10.5281/ZENODO.592483
[24] B. A. N. Couto and A. G. Casali. (2023) "gTRCA for Evoked Potentials," [Online]. Available: https://github.com/Boutoo/gTRCA
[25] H. Tanaka, T. Katura, and H. Sato, "Task-related component analysis for functional neuroimaging and application to near-infrared spectroscopy data," *NeuroImage*, vol. 64, pp. 308–327, Jan. 2013, doi: 10.1016/j.neuroimage.2012.08.044.
[26] H. Tanaka, T. Katura, and H. Sato, "Task-related oxygenation and cerebral blood volume changes estimated from NIRS signals in motor and cognitive tasks," *NeuroImage*, vol. 94, pp. 107–119, Jul. 2014, doi: 10.1016/j.neuroimage.2014.02.036.